

## THE DIVERSITY OF KILONOVA EMISSION IN SHORT GAMMA-RAY BURSTS

B. P. GOMPERTZ,<sup>1</sup> A. J. LEVAN,<sup>1</sup> N. R. TANVIR,<sup>2</sup> J. HJORTH,<sup>3</sup> S. COVINO,<sup>4</sup> P. A. EVANS,<sup>2</sup> A. S. FRUCHTER,<sup>5</sup>  
C. GONZÁLEZ-FERNÁNDEZ,<sup>6</sup> Z. JIN,<sup>7,8</sup> J. D. LYMAN,<sup>1</sup> S. R. OATES,<sup>1</sup> P. T. O'BRIEN,<sup>2</sup> AND K. WIERSEMA<sup>1</sup>

<sup>1</sup>*Department of Physics, University of Warwick, Coventry, CV4 7AL, UK*

<sup>2</sup>*Department of Physics and Astronomy, University of Leicester, Leicester, LE1 7RH, UK*

<sup>3</sup>*Dark Cosmology Centre, Niels Bohr Institute, University of Copenhagen, Juliane Maries Vej 30, 2100 Copenhagen, Denmark*

<sup>4</sup>*INAF, Osservatorio Astronomico di Brera, Via E. Bianchi 46, I-23807 Merate (LC), Italy*

<sup>5</sup>*Space Telescope Science Institute, 3700 San Martin Drive, Baltimore, MD 21218, USA*

<sup>6</sup>*Institute of Astronomy, University of Cambridge, Madingley Road, Cambridge, CB3 0HA, UK*

<sup>7</sup>*Key Laboratory of dark Matter and Space Astronomy, Purple Mountain Observatory, Chinese Academy of Science, Nanjing, 210008, China*

<sup>8</sup>*School of Astronomy and Space Science, University of Science and Technology of China, Hefei, Anhui 230026, China*

(Received; Revised; Accepted May 27, 2022)

Submitted to ApJ

### ABSTRACT

The historic first detection of gravitational wave emission from a binary neutron star merger by the advanced LIGO/Virgo detector network was also the inauguration of GW/EM multi-messenger astronomy, as an associated short gamma-ray burst (SGRB) and a radioactive kilonova (KN) were found in broad-band electromagnetic follow-up campaigns. These observations cement the association between SGRBs and compact object mergers, as well as providing a well sampled multi-wavelength light curve of a KN for the first time. Here we compare the optical and near-infrared light curves of this KN, AT2017gfo, to the counterparts of a sample of nearby ( $z < 0.5$ ) SGRBs to characterize their diversity in terms of their brightness distribution. Although at similar epochs AT2017gfo appears fainter than every SGRB-associated KN claimed so far, we find three bursts (GRBs 050509B, 061201 and 080905A) where, if the reported redshifts are correct, deep upper limits rule out the presence of a KN similar to AT2017gfo by several magnitudes. Combined with the properties of previously claimed KNe in SGRBs this suggests considerable diversity in the properties of KN drawn from compact object mergers, despite the similar physical conditions that are expected in many NS-NS mergers. This diversity is likely a product of the merger type (NS-NS versus NS-BH) and the detailed properties of the binary (mass ratio, spins etc). Ultimately disentangling these properties should be possible through observations of SGRBs and gravitational wave sources, providing direct measurements of heavy element enrichment throughout the Universe.

## 1. INTRODUCTION

Short gamma-ray bursts (SGRBs) have long been thought to be the products of the mergers of compact objects (Rosswog et al. 2003; Belczynski et al. 2006; Nakar 2007) - either a binary neutron star (BNS) or neutron star-black hole (NSBH) system. In this framework, the energy release of the merger launches relativistic jets that produce  $\gamma$ -rays in internal shocks. A broad-band synchrotron afterglow, with emission ranging from X-ray to radio frequencies, is then produced as the outflow decelerates in the circumstellar environment (Mészáros & Rees 1993). Such a merger is also expected to produce a faint optical/nIR transient known as a ‘kilonova’ (KN; or ‘macronova’) (Li & Paczyński 1998; Rosswog 2005; Metzger et al. 2010) as ejected material rich in neutrons forms heavy elements through rapid neutron capture (r-process) nucleosynthesis (Lattimer & Schramm 1974; Eichler et al. 1989; Freiburghaus et al. 1999) and subsequently decays radioactively. However, the discovery of GW 170817 (LIGO Scientific & Virgo Collaboration et al. 2017; LIGO Scientific Collaboration et al. 2017) by the Advanced Laser Interferometer Gravitational-Wave Observatory (LIGO) and Advanced Virgo provides the first direct evidence that the merger of a BNS has occurred. With it came the detection of SGRB 170817A by *Fermi* (Fermi-GBM 2017; Goldstein et al. 2017; von Kienlin et al. 2017) and later INTEGRAL (Savchenko et al. 2017). In broad-band follow-up observations (LIGO Scientific Collaboration et al. 2017), an optical transient (Coulter 2017a,b) identified as a KN, (AT2017gfo; e.g. Evans et al. 2017; Pian et al. 2017; Smartt et al. 2017; Tanvir et al. 2017) was detected, thus confirming the compact object merger origin for SGRBs and KNe.

Since 2005, the rapid localisations provided by the *Swift* satellite have meant that a catalogue of SGRB afterglows at multiple wavelengths has been established. However, KNe have been observed in just a handful of events: the first and best claim coming with SGRB 130603B (Tanvir et al. 2013; Berger et al. 2013), followed by a re-analysis of SGRBs 060614 (Yang et al. 2015) and 050709 (Jin et al. 2016), and an inconclusive fourth candidate in SGRB 160821B (Jin et al. 2017; Kasliwal et al. 2017). Interestingly, in GW 170817 no afterglow was detected after the *Fermi* trigger. Despite being tied to NGC 4993, a nearby early-type galaxy at  $z = 0.009783$ , or just 42.5 Mpc (Hjorth et al. 2017; Levan et al. 2017), no X-ray emission was detected down to  $2.7 \times 10^{-13}$  erg s $^{-1}$  cm $^{-2}$  at 0.62 days post-trigger (Evans et al. 2017). This is only reconcilable with an SGRB if the event was viewed off-axis - perhaps by as much as 30 degrees (Evans et al. 2017; Haggard et al. 2017; LIGO

Scientific Collaboration et al. 2017; Tanvir et al. 2017). This viewing geometry may have played a part in the identification of AT2017gfo, since due to their typical discovery via detection of the  $\gamma$ -ray jet, SGRBs are normally viewed down the jet axis where the afterglow is brightest and therefore most likely to mask a KN. KNe, however, are much more isotropic phenomena, and are therefore more easily detected at viewing angles away from the SGRB jet and the bright afterglow (Metzger & Berger 2012).

Through association with BNS mergers and KNe, SGRBs are now thought to be the site of a sizeable fraction of heavy element production in the Universe (Lattimer & Schramm 1974; Rosswog et al. 1998; Goriely et al. 2011; Korobkin et al. 2012; Just et al. 2015), supplementing the apparently insufficient yields predicted for supernovae (Burbidge et al. 1957). The identification of a clear KN signature accompanying GW 170817 and GRB 170817A provides the perfect opportunity to assess their general detectability in SGRBs and the variability in their properties. Known BNS in the Milky Way exist in a rather small range of total mass and mass ratio (Lattimer 2011; Tauris et al. 2017), and so one might naively expect them to drive similar KNe, which therefore ought to be reflected in the SGRB KN population if it is comprised entirely of BNS mergers. Alternatively, it might be that fine differences in the merging binaries or viewer orientation yields strongly differing observables, or that many SGRBs arise from NSBH rather than BNS mergers.

In this paper, we compare the optical and near-infrared light curves of the KN in GW 170817 to a sample of nearby ( $z \lesssim 0.5$ ) SGRBs to ascertain whether or not a KN of similar magnitude to AT2017gfo could (or even should) have been detected. We use a cosmology of  $H_0 = 67.8$  km s $^{-1}$  Mpc $^{-1}$ ,  $\Omega_M = 0.308$  and  $\Omega_\Lambda = 0.692$  (Planck Collaboration et al. 2016) throughout. All reported errors are  $1\sigma$ , and given upper limits are  $3\sigma$ .

## 2. AT2017gfo - THE KILONOVA ASSOCIATED WITH GW 170817

Our data for AT2017gfo come from Tanvir et al. (2017). We convert them to absolute magnitudes using a redshift of  $z = 0.009783$  (Hjorth et al. 2017; Levan et al. 2017).

To represent the evolution of AT2017gfo, we fit the light curves with Bazin functions (Bazin et al. 2011), which provide an estimate of rise ( $\tau_{\text{rise}}$ ) and decay ( $\tau_{\text{fall}}$ ) times by fitting the analytical function for a given band

$$f(t) = A \frac{e^{-(t-t_0)/\tau_{\text{fall}}}}{1 + e^{-(t-t_0)/\tau_{\text{rise}}}}, \quad (1)$$

| Band | $A$            | $t_0$ | $\tau_{\text{rise}}$ | $\tau_{\text{fall}}$ |
|------|----------------|-------|----------------------|----------------------|
|      | $\mu\text{Jy}$ | h     | h                    | h                    |
| r    | 544.50         | —     | —                    | 42.27                |
| y    | 752.86         | 11.52 | 14.05                | 74.17                |
| J    | 652.96         | 24.87 | 20.00                | 71.01                |
| K    | 635.33         | 58.20 | 27.21                | 109.87               |

**Table 1.** The best fits for AT2017gfo, taken in the observer frame. The y, J and K-bands are fitted with a Bazin function (Equation 1), while the r-band was better fitted with a simple exponential.

where  $A$  is the normalisation. Bazin et al. (2011) also present an additive constant,  $c$ , which we find to be zero in each case. We therefore re-fit with the constant excluded. Our fits are shown in Figure 1, while the fit parameters are given in Table 1.

These fits demonstrate the strongly chromatic behaviour of AT2017gfo. Indeed, the r-band shows no apparent peak within the span of our data, and declines from  $\sim 1.5$  days as a simple exponential decay. This decay is very different to the power-law seen in GRB afterglows, and coupled with the non-detection of X-rays at comparable times rules out an afterglow component brighter than an r-band absolute magnitude of  $M_r \sim -13$  at 0.62 days, assuming the mean r-band to X-ray flux ratio of 1130 found for SGRBs in Nysewander et al. (2009). Instead, the optical light is probably dominated by a rapidly fading transient created by the synthesis of lanthanide free ejecta, with relatively low opacity (Evans et al. 2017). The redder bands are not well explained by such a simple model, and indeed the light curves appear progressively broader as the observations move redward, and can be explained by a lanthanide-rich, higher opacity component (Tanvir et al. 2017).

### 3. SGRB DATA SAMPLE

We searched for nearby SGRBs with identified redshifts of  $z < 0.5$  in published works (Nysewander et al. 2009; Fong et al. 2015) and unpublished archives.<sup>1</sup> Our identified sample is shown in Table 2. Optical and IR photometric data are then collected from the published literature, or from GCN circulars. Any Vega magnitudes are converted to AB, and corrections for Galactic absorption are performed following the maps of Schlafly & Finkbeiner (2011) and using  $R_v = 3.1$  for the Milky Way. We do not make any corrections for extinction in the SGRB host galaxies.

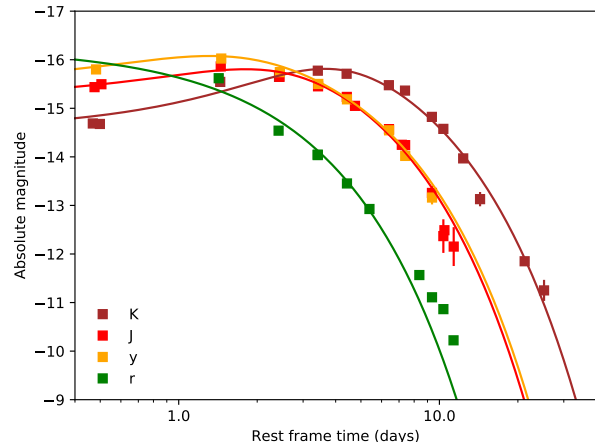


**Figure 1.** Model fit to AT2017gfo. The y, J and K-bands are fitted with a Bazin function, while the r-band is better fitted with a simple exponential. Error bars are smaller than the plot symbols in most cases.

In AT2017gfo it appears that the optical and IR light is dominated by the KN, at least for several days after the merger, and possibly for longer. Any afterglow component is very weak (Evans et al. 2017). However, in SGRBs the situation is very different. It is likely that most SGRBs are viewed close to the jet axis (see e.g. Ryan et al. 2015), and so show X-ray and optical afterglows. These afterglows probably dominate the light, at least for the first several days after the merger. However, the early, bright blue and UV emission from AT2017gfo also suggests that such KN may contribute here. Therefore, it is desirable to estimate the likely afterglow contribution in the optical bands at these times. We can do this by extrapolating the X-ray observations assuming standard afterglow behaviour.

*Swift* X-Ray Telescope (XRT) data are obtained for each SGRB from the 1 keV flux density light curves on the UK *Swift* Science Data Centre (UKSSDC) burst analyser<sup>2</sup> (Evans et al. 2007, 2009), except for SGRB 150101B, where we take the *Chandra* data from Fong et al. (2016) because the *Swift* light curve is dominated by the Active Galactic Nucleus (AGN) in the host galaxy. Additional X-ray data from *Chandra* and/or *XMM-Newton* are added for SGRBs 050709 (Fox et al. 2005), 050724 (Grupe et al. 2006), 130603B (Fong et al. 2014) and 140903A (Troja et al. 2016). We correct the *Swift* data for absorption using a ratio of [counts-to-flux unabsorbed]/[counts-to-flux observed], which we obtain from the automatically generated late-time pho-

<sup>1</sup> www.mpe.mpg.de/~jcg/grbgen.html

<sup>2</sup> www.swift.ac.uk/burst\_analyser/

| GRB     | $z$    | References     | GRB     | $z$   | References                 |
|---------|--------|----------------|---------|-------|----------------------------|
| 050509B | 0.2248 | 1, 2, 3        | 090515  | 0.403 | 28, 29, 30, 31, 32, 33     |
| 050709  | 0.161  | 4, 5, 6, 7     | 100206A | 0.407 | 26, 34, 35, 36, 37, 38, 39 |
| 050724  | 0.257  | 8, 9           | 100625A | 0.452 | 26, 40, 41, 42             |
| 051210  | 0.114  | 10, 11         | 130603B | 0.356 | 43, 44, 45, 46             |
| 060502B | 0.287  | 12, 13, 14     | 140903A | 0.351 | 47                         |
| 060614  | 0.125  | 15             | 150101B | 0.134 | 48, 49                     |
| 061006  | 0.438  | 16             | 150120A | 0.46  | 50, 51                     |
| 061201  | 0.084  | 17             | 150424A | 0.3   | 52, 53, 54, 55, 56         |
| 061210  | 0.41   | 18, 19, 20     | 160624A | 0.483 | 57, 58, 59                 |
| 070724A | 0.457  | 21, 22, 23     | 160821B | 0.16  | 60, 61                     |
| 071227  | 0.384  | 16, 24, 25, 26 | 170428A | 0.454 | 62, 63, 64                 |
| 080905A | 0.1218 | 26, 27         | —       | —     | —                          |

**Table 2.** The sample of SGRBs with their redshifts,  $z$ , and the source of their photometry.

(1) - Castro-Tirado et al. (2005); (2) - Hjorth et al. (2005a); (3) - Bloom et al. (2006); (4) - Fox et al. (2005); (5) - Hjorth et al. (2005b); (6) - Covino et al. (2006); (7) - Jin et al. (2016); (8) - Berger et al. (2005); (9) - Malesani et al. (2007); (10) - Blustin et al. (2005); (11) - Berger & Boss (2005); (12) - Poole & Troja (2006); (13) - Price et al. (2006); (14) - Rumyantsev et al. (2006); (15) - Yang et al. (2015); (16) - D’Avanzo et al. (2009); (17) - Stratta et al. (2007); (18) - Melandri et al. (2006); (19) - Mirabal & Halpern (2006); (20) - Cenko et al. (2006); (21) - Cenko et al. (2007); (22) - Berger et al. (2009); (23) - Kocevski et al. (2010); (24) - D’Avanzo et al. (2007); (25) - Berger et al. (2007); (26) - Nicuesa Guelbenzu et al. (2012); (27) - Rowlinson et al. (2010); (28) - Morgan et al. (2009); (29) - Utdike et al. (2009); (30) - Cucchiara et al. (2009); (31) - Siegel & Beardmore (2009); (32) - McLeod & Williams (2009); (33) - Perley et al. (2009); (34) - Leloudas et al. (2010); (35) - Kuroda et al. (2010); (36) - Marshall & Krimm (2010); (37) - Berger & Chornock (2010); (38) - Andreev et al. (2010); (39) - Rumyantsev et al. (2010); (40) - Naito et al. (2010); (41) - Landsman & Holland (2010); (42) - Fong et al. (2013); (43) - Tanvir et al. (2013); (44) - Cucchiara et al. (2013); (45) - de Ugarte Postigo et al. (2014); (46) - Fong et al. (2014); (47) - Troja et al. (2016); (48) - D’Avanzo et al. (2015); (49) - Fong et al. (2016); (50) - Chornock & Fong (2015); (51) - Chester & D’Elia (2015); (52) - Marshall & Beardmore (2015); (53) - Malesani et al. (2015); (54) - Kann et al. (2015); (55) - Butler et al. (2015); (56) - Knust et al. (2017); (57) - Kuroda et al. (2016); (58) - Kong et al. (2016); (59) - de Pasquale & D’Ai (2016); (60) - Jin et al. (2017); (61) - Kasliwal et al. (2017); (62) - Kuin & Beardmore (2017); (63) - Bolmer et al. (2017); (64) - Troja et al. (2017).

ton counting mode spectral fit in the XRT spectrum repository on the UKSSDC website. The flux densities are converted to AB magnitudes and extrapolated to 6260Å (r-band) for easy comparison with the optical data. The assumed spectral indices of the extrapolation are  $\beta = 0.5$ , which represents the case in which the synchrotron cooling break is above the X-ray frequency, and  $\beta = 1.0$ , which implies the synchrotron cooling break is down near optical frequencies. Both of these assume that the electron energies follow a power-law distribution with an index of  $p = 2$ , which is the theoretically expected value (Sari et al. 1998). In nature, measurements of spectral and temporal indices often imply that this distribution is steeper than  $p = 2$  (e.g. Curran et al. 2010), suggesting that a steeper spectral index would be needed. However, the synchrotron cooling break is typically measured to be somewhere close to X-ray frequencies rather than in the optical part of the spectrum (e.g. Gompertz et al. 2015), so flux densities bracketed by our two extrapolations provide a reason-

able estimation of where the SGRB afterglow should occur.

We convert all apparent magnitudes to absolute magnitudes, assuming for a given band  $k$ ,  $k_{abs} = k_{AB} - 5 \log_{10}(d_L/10\text{pc}) + 2.5 \log_{10}(1 + z)$ . Observed times are divided by  $(1 + z)$  to put them in the rest frame. We do not correct for the redshift of the central frequency of the photometric filter because this would require assuming a spectral shape that is uncertain in many SGRBs. Instead we interpolate and shift the well sampled lightcurve of AT2017gfo to the rest frame wavelength represented by the observations (see below). This means our photometry is presented in its observer frame band, such that the magnitudes are given at  $\lambda_k = (1 + z)\lambda_r$ , where  $\lambda_r$  is the rest frame emitting wavelength. Since KNe do not appear (or are at least very weak) at X-ray frequencies, this issue does not affect our X-ray extrapolations.

While the optical to IR spectral energy distributions of our SGRBs are usually poorly constrained, we do



have good colour coverage of AT2017gfo. We therefore adjust our model fits to the wavelengths of the SGRB observations via linear interpolations between the fitted curves in Figure 1. Where the rest-frame frequency is bluewards of the r-band fit to AT2017gfo, we supplement with observations with the *Swift*-UVOT u-band data from Evans et al. (2017) and the HST F475W (g-band) data from Tanvir et al. (2017), with an early g-band point based on the spectral flux density measured in our MUSE spectroscopy. We fit both datasets with an exponential decay to ascertain the required colour correction. Fitting in the observer frame, we find  $A_g = 321.92 \mu\text{Jy}$ ,  $\tau_{g,fall} = 39.10$  hours, and  $A_u = 321.39 \mu\text{Jy}$ ,  $\tau_{u,fall} = 20.25$  hours. We note that these bands have only a small number (3-4) points to fit, and so we have assumed they follow an exponential decay as the r-band does, but do not have sufficient data discriminate between alternative models. We do not extrapolate beyond the u-band if the rest-frame wavelength is less than  $3560\text{\AA}$ .

#### 4. RESULTS

Light curves of our results are shown in Figure 2. We find that for several SGRBs, a KN as bright as AT2017gfo could have been detected. Most notably, GRBs 050509B, 061201 and 080905A have upper limits several magnitudes deeper than the detections of AT2017gfo at similar rest-frame times. GRB 080905A is the most constraining case, as its r-band limit is about 4.5 times deeper than the r-band light curve of AT2017gfo. In SGRB 050509B, the r-band limits are over 3 times deeper than the r-band model curve in AT2017gfo. They therefore represent cases in which a KN similar to AT2017gfo could have been detected if it was present. SGRB 061201 has i-band limits that are more than a factor of 4 deeper than the i-band model for AT2017gfo. It also has an X-ray afterglow extrapolation that is fainter than AT2017gfo. Both of these facts suggest that a AT2017gfo-like KN could have been detected. These limits assume that in each case the redshift of the burst is correctly ascribed, and this is considered in more detail in section 5. Other SGRBs with upper limits of comparable absolute magnitudes to the AT2017gfo detection are 051210, which has an i-band upper limit 2 times deeper than the AT2017gfo model, and 060502B, where the limits are 2.5 times shallower. The latter is not deep enough to rule out a AT2017gfo-like event, though the former marginally could.

Compared to the SGRB KN candidates, AT2017gfo appears to be faint. The H-band detection in GRB 130603B is almost 3 times brighter than the interpolated KN model fit at the time of the observation. Similarly

in SGRB 050709, the K-band detection is far brighter than the K-band of GW 170817. However, the i-band light curve appears to be fainter and peak later than AT2017gfo, though the photometry is limited. The afterglow of GRB 060614 is already much brighter than the light curve of AT2017gfo, and the i-band photometric excess (Yang et al. 2015) is over 50 times brighter than the contemporary KN fit, though it could be a later/longer rise like SGRB 050709. Alternatively, as shown in Figure 1, the extrapolation of the X-ray afterglow to optical/IR wavelengths may imply significant afterglow contributions at this time, such that the KN components can be fainter. The photometric excess claimed by Jin et al. (2017) in 160821B is the only potential KN less bright than AT2017gfo, though the data are inconclusive in this case (see Tanvir et al. in prep. for a detailed analysis of this burst).

Finally, we identify several SGRBs in which the afterglow was likely too bright for a AT2017gfo-like KN to be detected. SGRB 150424A has optical/nIR afterglow detections several magnitudes brighter than AT2017gfo, and its detections and limits are never less than about 3 times brighter than the relevant model light curve in the H-band, or 10 times in the r-band. SGRBs 140903A and 150101B have extrapolated X-ray afterglows that are brighter than AT2017gfo, with optical detections that support the extrapolation, though there are no nIR limits constraining a redder transient. The i-band detection in SGRB 140903A is almost 15 times brighter than the AT2017gfo model. The r-band detection in SGRB 150101B is just 2 times the flux of the AT2017gfo model, so could potentially have a KN contribution, indeed it is notable that its decay between the two epochs of observations is very similar to AT2017gfo. SGRB 050724 features a large flare seen in X-ray, nIR and optical bands. The i-band detection close to 3 days is of a similar brightness to the one in 060614 (which was identified as a KN by its i-band excess; Yang et al. 2015), but the contribution from the various emission features is unknown.

SGRB 061210 has an extrapolated X-ray afterglow that would be bright enough to mask a similar KN if accurate. SGRB 070724A has an extrapolated X-ray afterglow similar to that of SGRB 130603B, but its deepest observation is an i-band limit that reaches 4 times the flux of the contemporaneous model. SGRBs 061006, 071227 and 170428A all lie on bright host galaxies, making KN detection impossible.

#### 5. DISCUSSION

We search our sample of 23 SGRBs with identified redshift of  $z < 0.5$  and optical/nIR observations for

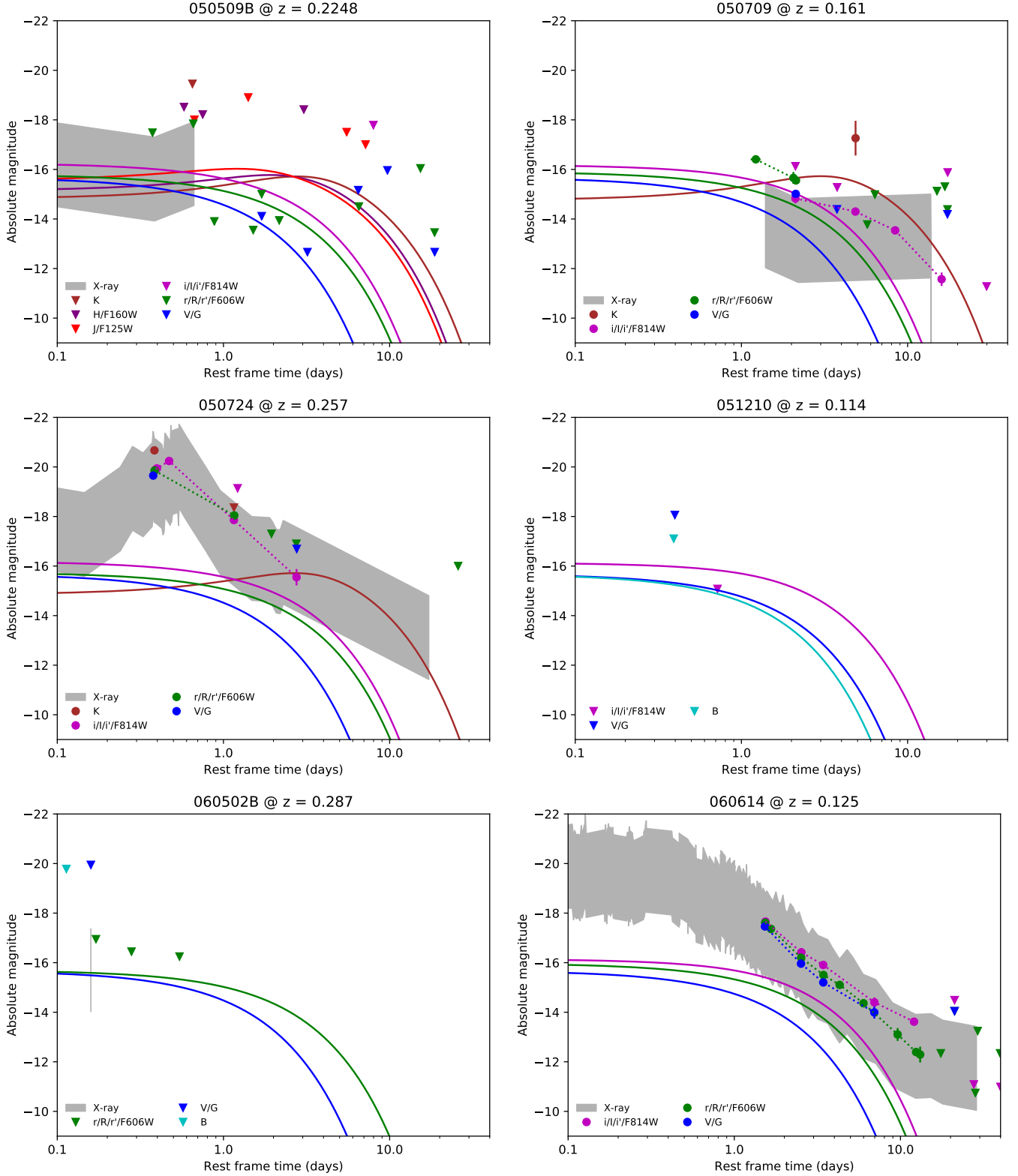


**Figure 2.** Our sample of SGRB afterglows compared to the model fits of AT2017gfo. Coloured circles are detections, and triangles are upper limits. These data are presented in their observer frame filters, and the AT2017gfo models (coloured lines) are shifted in frequency to match them using linear interpolation of the fits in Figure 1 supplemented by the g-band data from Tanvir et al. (2017) and the u-band data from Evans et al. (2017). We do not extrapolate if the rest-frame wavelength is below the u-band ( $3560\text{\AA}$ ), so some data do not have models plotted. The grey band is the extrapolation of the X-ray flux to  $6260\text{\AA}$  (r-band). SGRBs from Table 2 with no constraining observations are not included.

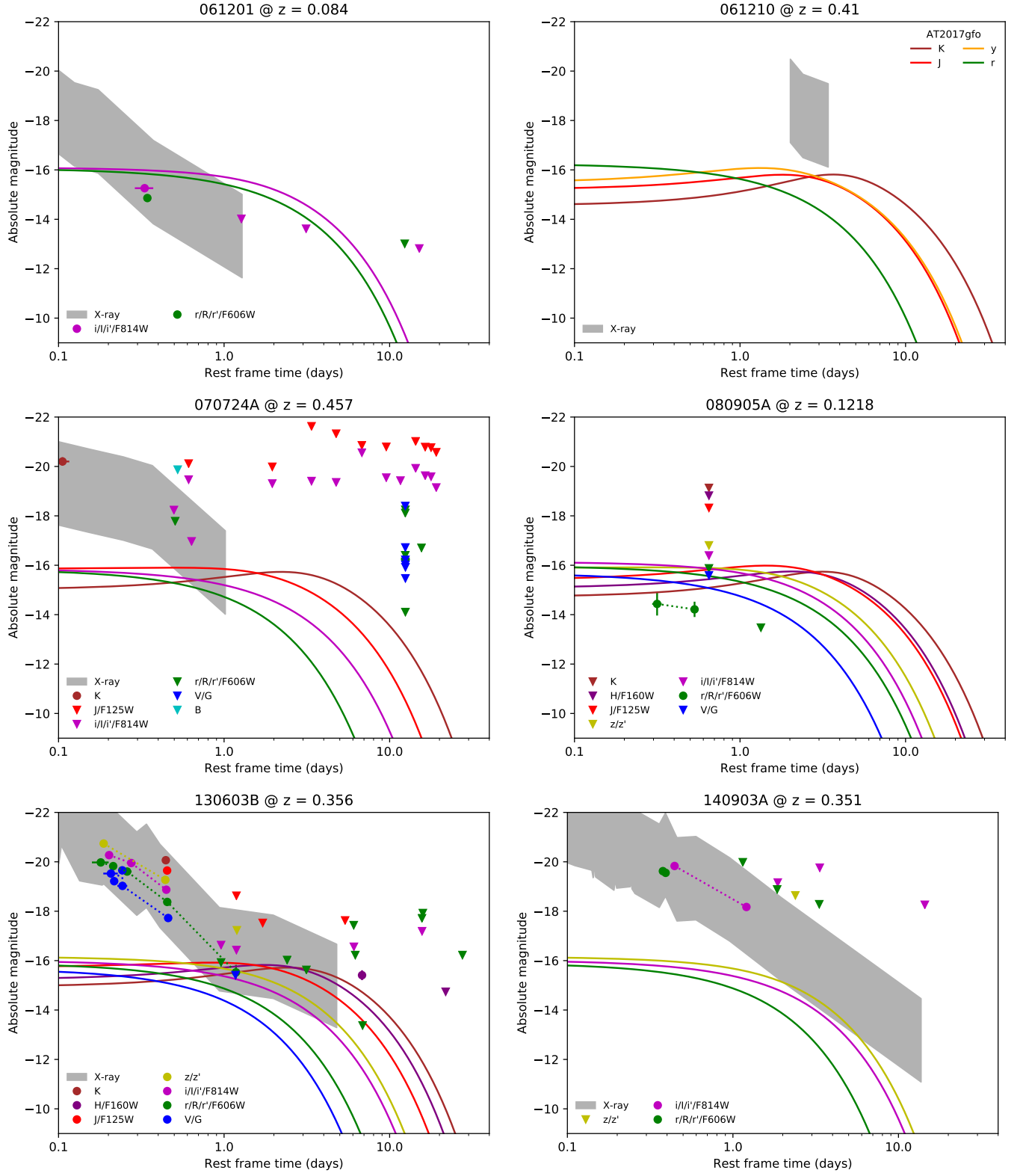


Figure 2. continued

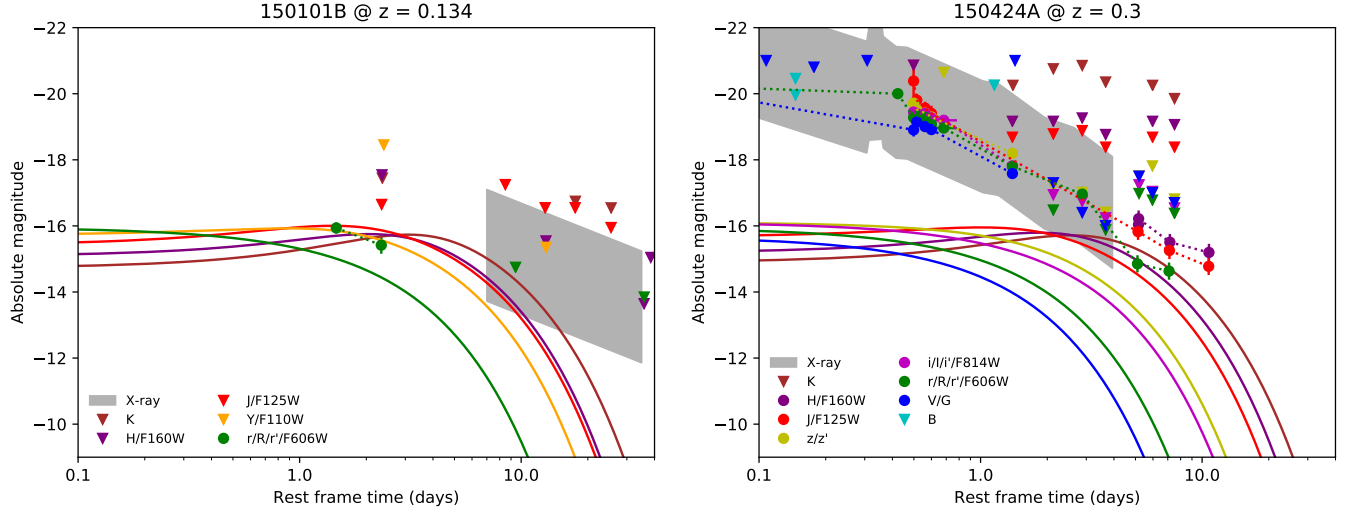


Figure 2. continued

detections and limits constraining to KNe similar to AT2017gfo, or bright afterglows capable of masking a KN of this magnitude. 3 have claimed KNe in the literature (050709, 060614, 130603B) with a further marginal case (160821B; see Tanvir et al. in prep. for a detailed analysis). 4 have limits deeper than AT2017gfo (050509B, 051210, 061201, 080905A), and 3 of these are over a magnitude deeper (050509B, 061201, 080905A). 1 more has limits of comparable depth (060502B). 4 have bright detected optical/nIR afterglows consistent with the light arising from an afterglow component (050724, 140903A, 150101B, 150424A), although at least in one case an magnitude only marginally brighter than AT2017gfo (GRB 150101B). 2 have afterglows that are implied to be bright by the X-ray extrapolation (061210, 070724A), although were in fact not observed. 3 have bright host galaxies (061006, 071227, 170428A), and the remaining 5 are completely unconstrained by the available observations. The broad range of magnitudes in the sample suggests a diversity in the brightness of KNe associated with SGRBs.

For three bursts in particular, the absence of a KN is conspicuous. SGRBs 050509B, 061201 and 080905A all have limits much deeper than the detections for AT2017gfo, and any KN would have had to have been at least five times fainter to be missed, yet AT2017gfo itself is fainter than any KN seen in SGRBs so far.

There are two concerns that should be addressed in interpreting these limits. The first is whether the measured magnitudes are indeed indicative of the intrinsic luminosity of the KN, or if there could be some unseen extinction along the line of sight. In the case of GRB 050509B this is a concern since there is no optical light at any epoch, and too few X-ray photons to determine a

column density. For GRB 061201 and 080905A the detection of the sources in optical light rules out extreme extinction, but does not discount moderate levels. Fong et al. (2015) find that both of these bursts are consistent with having no host extinction in their modelling.

It is notable in these examples that the optical light is consistent with the X-ray extrapolation (where available) with  $\beta = 0.5$ , and so the bursts are not “dark” GRBs (Jakobsson et al. 2004).

The second concern is the validity of the assumed redshifts. Only one short GRB has a redshift measured in absorption, GRB 130603B (de Ugarte Postigo et al. 2014), in other cases the redshifts are based on putative host galaxy identifications. For GRB 050509B there is a large cD galaxy close to the location, and a coincidence with a massive, merging galaxy cluster. Much of the mass along this line of sight lies within this cluster, and the redshift has high confidence (see e.g. Bloom et al. 2002; Levan et al. 2007). For GRB 080905A the burst position overlaps the spiral arm of the host galaxy, again suggesting a chance alignment probability of  $\lesssim 1\%$ . However, for GRB 061201 the situation is more complex. The burst belongs to the so-called hostless SGRB population (Berger 2010; Tunnicliffe et al. 2014), and so the redshift is based on a proximity to the Abell 995 cluster (Berger 2006; Stratta et al. 2007). This is a rich cluster, but there are no galaxies within a few arcseconds of the burst position, and so the probability of chance a alignment is significant, and the redshift should be viewed with caution. While the probabilities of any given burst redshift being wrong appear small, it should also be noted that assigning redshifts by probabilistic arguments favours the brightest nearby galaxies, many of which are likely to be closer, and so this may



produce a bias in which incorrect host assignments, lead to lower redshifts, and hence strong KN constraints.

The SGRBs with bright afterglows still may have KN contributions in the detected flux. The inferred contribution from an AT2017gfo-like KN ranges from 1/15 (140903A) to 1/2.5 (150101B), and the latter end of the scale is certainly enough to cause a spectral energy distribution (SED) to deviate away from the power law expected from the synchrotron afterglow. A KN was discovered this way for both SGRBs 050709 (Jin et al. 2016) and 060614 (Yang et al. 2015), and potentially 160821B too (Jin et al. 2017). However, no multi-colour observations are available for any of these bursts except 150424A, the brightest of the four. Jin et al. (2017) found no evidence of chromatic deviation in this source.

AT2017gfo appears to be somewhat fainter than other established KN, but the lack of X-ray afterglow to deep limits ( $2.7 \times 10^{-13} \text{ erg s}^{-1} \text{ cm}^{-2}$  at 0.62 days after trigger; Evans et al. 2017) suggests that the viewing angle is further off-axis than in typical SGRBs - perhaps up to 30 degrees away from the jet axis (Evans et al. 2017; Haggard et al. 2017; LIGO Scientific Collaboration et al. 2017; Tanvir et al. 2017). The fainter KN in GW 170817 is therefore within the variation expected from the observer position (e.g. Grossman et al. 2014). The peak time and luminosity of a KN is also a function of ejecta mass and opacity (e.g. Metzger et al. 2010), and naturally some variation is expected from case to case.

### 5.1. Rates

Recent work on the SGRB luminosity function provides a rate of mergers within 200 Mpc of  $\sim 7 \times 10^{-3} \text{ yr}^{-1}$  (or one per 140 years Ghirlanda et al. 2016), or a volumetric rate of  $R_{\text{SGRB}} \sim 0.2 \text{ Gpc}^{-3} \text{ yr}^{-1}$ . At first sight it appears rather unlikely to have observed a GW trigger and SGRB from a galaxy within 40 Mpc during the second LIGO observing run (O2). However, SGRB 170817A appears to have been unusually low luminosity, KN modelling suggests a modestly off-axis event (Evans et al. 2017; Haggard et al. 2017; LIGO Scientific Collaboration et al. 2017; Tanvir et al. 2017), and this may remove this concern. Indeed, since it is widely believed that SGRBs are beamed it is natural that the true rate is greater than the observed one by the beaming factor  $f_b \sim 2/\theta_j^2$ . For opening angles in the region of 5-10 degrees the beaming factor is 50-250, and so doesn't create any obvious tension with the observation of an event in O2.

We can now turn our attention to the implications of mergers at the measured SGRB rate, in particular for the enrichment of the interstellar and intergalactic medium. To do this, we can take both an extremely con-

servative, and more realistic view. There is reasonable evidence for KN-like emission in at least 4 bursts (GRBs 050709, 060614, 130603B, 160821B), in most cases somewhat brighter than AT2017gfo. The most conservative estimate would be to assume that each of these events ejected perhaps  $M_{ej} \sim 10^{-2} M_{\odot}$  of r-process material. If such KNe are present in only  $\sim 25\%$  of SGRBs (and others produce none) then the r-process yield will be  $0.25 M_{ej} R_{\text{SGRB}} f_b$ .

Within this  $f_b$  remains the largest uncertainty, but is one that will be removed by future GW observations. For the extremely conservative  $f_b = 1$  the total mass ejection is  $\dot{M} = 5 \times 10^{-4} M_{\odot} \text{ yr}^{-1} \text{ Gpc}^{-3}$  or  $\dot{M}_{\text{gal}} = 4 \times 10^{-11} M_{\odot} \text{ yr}^{-1}$  using the conversion rate of Abadie et al. (2010). This is well below the necessary rate of injection to explain the r-process abundances in the Milky Way of  $\sim 10^{-7} M_{\odot} \text{ yr}^{-1}$  (Macias & Ramirez-Ruiz 2016). Alternatively, if every burst created  $M_{ej} \sim 10^{-2} M_{\odot}$ , and the beaming factor was 250, then the rate would be  $\sim 4 \times 10^{-8} M_{\odot} \text{ yr}^{-1}$ , and given other systematic uncertainties (for example of the true  $R_{\text{SGRB}}$ , or on contributions from BNS and NSBH mergers, the latter of which can produce up to 10 times as much dynamical ejecta; Metzger 2017), it is likely that such events could provide the necessary material to explain the observed r-process yields.

It should also be noted that SGRBs probe the KN emission from a unique, face-on, angle. While KNe are typically described as isotropic counterparts to binary mergers, they are in fact, not isotropic events, since they are produced by nucleosynthesis in material ejected in a disc wind, or in tidal tails (for measurements of the geometry and isotropy of AT2017gfo, see Covino et al. 2017). This geometry allows for viewing in all directions, so KNe can be seen isotropically, but they may differ greatly depending on the angle (e.g. Grossman et al. 2014). Hence, while SGRBs provide one view, the KNe seen in association with only gravitational wave triggers might lead to a different conclusion.

## 6. CONCLUSIONS

Our analysis reveals a diverse range of KN possibilities, as in some SGRBs we find upper limits for optical/nIR emission several magnitudes deeper than AT2017gfo, in others there are identified (or suspected) KNe that are brighter, and we also find SGRBs with bright afterglows capable of masking KNe that are brighter still. Our sample spans five magnitudes at a few days after trigger (Figure 3). The most interesting comparison is between the SGRBs with detected KNe (including AT2017gfo) and the 3 SGRBs with deep limits; the diversity between these two groups is hard to

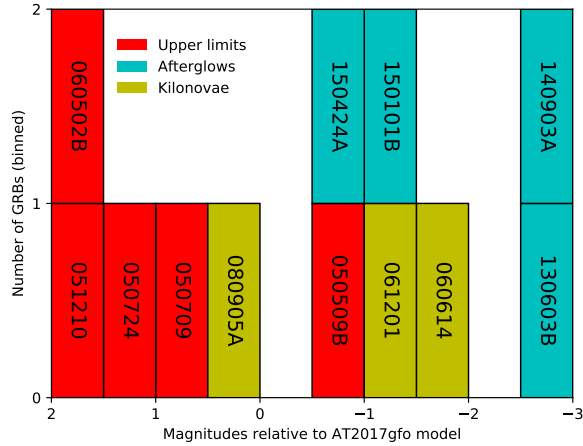


**Figure 3.** A snapshot of the i/r-band magnitudes of our SGRB observations relative to the AT2017gfo models, taken between 0.5 and 3 days after trigger. Data are binned into 0.5 magnitude intervals. Bursts with upper limits not constraining to the AT2017gfo models are not included.

reconcile with the highly uniform distribution of known BNS masses and mass ratios in the Milky Way (Lattimer 2011; Tauris et al. 2017).

The relatively small range of viewing angles in the SGRB population means that the observer position alone probably can’t explain the  $\sim 3.5$  magnitudes (a factor of 25 in flux) between the KN in SGRB 060614 and the upper limits in SGRBs 061201 and 080905A. If their redshifts are correct, they may potentially suggest a BNS/NSBH dichotomy in the SGRB population, as this represents the most natural way to explain an ap-

parent contrast in the ejected masses available to power a KN; an NSBH merger can produce as much as 10 times more dynamical ejecta than can a BNS (Metzger 2017).

The LIGO/Virgo detection of GW 170817 (LIGO Scientific Collaboration et al. 2017; LIGO Scientific & Virgo Collaboration et al. 2017) and electromagnetic follow-up and identification of SGRB 170717A (Fermi-GBM 2017; Goldstein et al. 2017; von Kienlin et al. 2017; Savchenko et al. 2017) and AT2017gfo (Coulter 2017a,b; Evans et al. 2017; Pian et al. 2017; Smartt et al. 2017; Tanvir et al. 2017) brings about the advent of KN astronomy. Further observations of KNe will reveal whether the magnitude of the emission forms a continuum, or continues to display a gap in brightness between two populations. Unsurprisingly, our best constraints come from the SGRBs at the lowest redshifts, and our work emphasises the need to perform KN searches at low  $z$  and in nIR filters.

AJL, JDL acknowledge support from STFC via grant ST/P000495/1. BG, AJL, NRT & KW have received funding from the European Research Council (ERC) under the European Union’s Horizon 2020 research and innovation programme (grant agreement no 725246, TEDE, PI Levan).

JH was supported by a VILLUM FONDEN Investigator grant (project number 16599).

SC acknowledges partial funding from Agenzia Spaziale Italiana-Istituto Nazionale di Astrofisica grant I/004/11/3.

SRO gratefully acknowledges the support of the Leverhulme Trust Early Career Fellowship. This work made use of data supplied by the UK Swift Science Data Centre at the University of Leicester.

## REFERENCES

- Abadie, J., Abbott, B. P., Abbott, R., et al. 2010, *Classical and Quantum Gravity*, 27, 173001
- Andreev, M., Sergeev, A., Parakhin, N., et al. 2010, *GRB Coordinates Network*, Circular Service, No. 10455, #1 (2010), 10455
- Bazin, G., Ruhlmann-Kleider, V., Palanque-Delabrouille, N., et al. 2011, *A&A*, 534, A43
- Belczynski, K., Perna, R., Bulik, T., et al. 2006, *ApJ*, 648, 1110
- Berger, E. 2006, *GRB Coordinates Network*, 5952
- . 2010, *ApJ*, 722, 1946
- Berger, E., & Boss, A. 2005, *GRB Coordinates Network*, 4323
- Berger, E., Cenko, S. B., Fox, D. B., & Cucchiara, A. 2009, *ApJ*, 704, 877
- Berger, E., & Chornock, R. 2010, *GRB Coordinates Network*, Circular Service, No. 10410, #1 (2010), 10410
- Berger, E., Fong, W., & Chornock, R. 2013, *ApJL*, 774, L23
- Berger, E., Morrell, N., & Roth, M. 2007, *GRB Coordinates Network*, 7151
- Berger, E., Price, P. A., Cenko, S. B., et al. 2005, *Nature*, 438, 988
- Bloom, J. S., Kulkarni, S. R., & Djorgovski, S. G. 2002, *AJ*, 123, 1111
- Bloom, J. S., Prochaska, J. X., Pooley, D., et al. 2006, *ApJ*, 638, 354
- Blustin, A. J., Mangano, V., Voges, W., Marshall, F., & Gehrels, N. 2005, *GRB Coordinates Network*, 4331
- Bolmer, J., Steinle, H., & Schady, P. 2017, *GRB Coordinates Network*, Circular Service, No. 21050, #1 (2017), 21050

- Burbidge, E. M., Burbidge, G. R., Fowler, W. A., & Hoyle, F. 1957, *Reviews of Modern Physics*, 29, 547
- Butler, N., Watson, A. M., Kutyrev, A., et al. 2015, GRB Coordinates Network, Circular Service, No. 17762, #1 (2015), 17762
- Castro-Tirado, A. J., de Ugarte Postigo, A., Gorosabel, J., et al. 2005, *A&A*, 439, L15
- Cenko, S. B., Fox, D. B., & Price, P. A. 2006, GRB Coordinates Network, 5912
- Cenko, S. B., Rau, A., Berger, E., Price, P. A., & Cucchiara, A. 2007, GRB Coordinates Network, 6664
- Chester, M. M., & D’Elia, V. 2015, GRB Coordinates Network, Circular Service, No. 17323, #1 (2015), 17323
- Chornock, R., & Fong, W. 2015, GRB Coordinates Network, Circular Service, No. 17358, #1 (2015), 17358
- Coulter, D. A. e. a. 2017a, GRB Coordinates Network, 21529
- . 2017b, *Science*, doi:10.1126/science.aap9811
- Covino, S., Wiersema, K., Fan, Y. Z., et al. 2017, doi:10.1038/s41550-017-0285-z
- Covino, S., Malesani, D., Israel, G. L., et al. 2006, *A&A*, 447, L5
- Cucchiara, A., Fox, D. B., Tanvir, N., et al. 2009, GRB Coordinates Network, 9362
- Cucchiara, A., Prochaska, J. X., Perley, D., et al. 2013, *ApJ*, 777, 94
- Curran, P. A., Evans, P. A., de Pasquale, M., Page, M. J., & van der Horst, A. J. 2010, *ApJL*, 716, L135
- D’Avanzo, P., D’Elia, V., Lorenzi, V., et al. 2015, GRB Coordinates Network, Circular Service, No. 17326, #1 (2015), 17326
- D’Avanzo, P., Piranomonte, S., Antonelli, L. A., et al. 2007, GRB Coordinates Network, 7149
- D’Avanzo, P., Malesani, D., Covino, S., et al. 2009, *A&A*, 498, 711
- de Pasquale, M., & D’Ai, A. 2016, GRB Coordinates Network, Circular Service, No. 19576, #1 (2016), 19576
- de Ugarte Postigo, A., Thöne, C. C., Rowlinson, A., et al. 2014, *A&A*, 563, A62
- Eichler, D., Livio, M., Piran, T., & Schramm, D. N. 1989, *Nature*, 340, 126
- Evans, P. A., Cenko, S. B., Kennea, J. A., et al. 2017, doi:10.1126/science.aap9580
- Evans, P. A., Beardmore, A. P., Page, K. L., et al. 2007, *A&A*, 469, 379
- . 2009, *MNRAS*, 397, 1177
- Fermi-GBM. 2017, GRB Coordinates Network, 524666471
- Fong, W., Berger, E., Margutti, R., & Zauderer, B. A. 2015, *ApJ*, 815, 102
- Fong, W., Berger, E., Chornock, R., et al. 2013, *ApJ*, 769, 56
- Fong, W., Berger, E., Metzger, B. D., et al. 2014, *ApJ*, 780, 118
- Fong, W., Margutti, R., Chornock, R., et al. 2016, *ApJ*, 833, 151
- Fox, D. B., Frail, D. A., Price, P. A., et al. 2005, *Nature*, 437, 845
- Freiburghaus, C., Rosswog, S., & Thielemann, F.-K. 1999, *ApJL*, 525, L121
- Ghirlanda, G., Salafia, O. S., Pescalli, A., et al. 2016, *A&A*, 594, A84
- Goldstein et al. 2017, *ApJL*, doi:doi.org/10.3847/2041-8213/aa8f41
- Gompertz, B. P., van der Horst, A. J., O’Brien, P. T., Wynn, G. A., & Wiersema, K. 2015, *MNRAS*, 448, 629
- Goriely, S., Bauswein, A., & Janka, H.-T. 2011, *ApJL*, 738, L32
- Grossman, D., Korobkin, O., Rosswog, S., & Piran, T. 2014, *MNRAS*, 439, 757
- Grupe, D., Burrows, D. N., Patel, S. K., et al. 2006, *ApJ*, 653, 462
- Haggard et al. 2017, doi:10.3847/2041-8213/aa8ede
- Hjorth, J., Levan, A. J., Tanvir, N. R., et al. 2017, *ApJL*, doi:10.3847/2041-8213/aa9110
- Hjorth, J., Sollerman, J., Gorosabel, J., et al. 2005a, *ApJL*, 630, L117
- Hjorth, J., Watson, D., Fynbo, J. P. U., et al. 2005b, *Nature*, 437, 859
- Jakobsson, P., Hjorth, J., Fynbo, J. P. U., et al. 2004, *ApJL*, 617, L21
- Jin, Z.-P., Hotokezaka, K., Li, X., et al. 2016, *Nature Communications*, 7, 12898
- Jin, Z.-P., Li, X., Wang, H., et al. 2017, *ArXiv e-prints*, arXiv:1708.07008
- Just, O., Bauswein, A., Pulpillo, R. A., Goriely, S., & Janka, H.-T. 2015, *MNRAS*, 448, 541
- Kann, D. A., Tanga, M., & Greiner, J. 2015, GRB Coordinates Network, Circular Service, No. 17757, #1 (2015), 17757
- Kasliwal, M. M., Korobkin, O., Lau, R. M., Wollaeger, R., & Fryer, C. L. 2017, *ApJL*, 843, L34
- Knust, F., Greiner, J., van Eerten, H. J., et al. 2017, *ArXiv e-prints*, arXiv:1707.01329
- Kocevski, D., Thöne, C. C., Ramirez-Ruiz, E., et al. 2010, *MNRAS*, 404, 963
- Kong, A. K. H., Lee, M. Y., Lin, Y.-M., Hou, X., & Liu, C. Y. 2016, GRB Coordinates Network, Circular Service, No. 19575, #1 (2016), 19575

- Korobkin, O., Rosswog, S., Arcones, A., & Winteler, C. 2012, *MNRAS*, 426, 1940
- Kuin, N. P. M., & Beardmore, A. P. 2017, GRB Coordinates Network, Circular Service, No. 21049, #1 (2017), 21049
- Kuroda, D., Yanagisawa, K., Shimizu, Y., et al. 2010, GRB Coordinates Network, Circular Service, No. 10388, #1 (2010), 10388
- Kuroda, D., Hanayama, H., Miyaji, T., et al. 2016, GRB Coordinates Network, Circular Service, No. 19571, #1 (2016), 19571
- Landsman, W., & Holland, S. 2010, GRB Coordinates Network, Circular Service, No. 10892, #1 (2010), 10892
- Lattimer, J. M. 2011, *Ap&SS*, 336, 67
- Lattimer, J. M., & Schramm, D. N. 1974, *ApJL*, 192, L145
- Leloudas, G., Xu, D., Malesani, D., et al. 2010, GRB Coordinates Network, Circular Service, No. 10387, #1 (2010), 10387
- Levan, A. J., Lyman, J. D., Tanvir, N. R., et al. 2017, doi:10.3847/20418213/
- Levan, A. J., Jakobsson, P., Hurkett, C., et al. 2007, *MNRAS*, 378, 1439
- Li, L.-X., & Paczyński, B. 1998, *ApJL*, 507, L59
- LIGO Scientific, & Virgo Collaboration et al. 2017, GRB Coordinates Network, 21505
- LIGO Scientific Collaboration, Virgo Collaboration, & Partner Astronomy Groups. 2017, doi:10.1103/PhysRevLett.119.161101
- Macias, P., & Ramirez-Ruiz, E. 2016, *ArXiv e-prints*, arXiv:1609.04826
- Malesani, D., Xu, D., Watson, D. J., & Blay, P. 2015, GRB Coordinates Network, Circular Service, No. 17756, #1 (2015), 17756
- Malesani, D., Covino, S., D’Avanzo, P., et al. 2007, *A&A*, 473, 77
- Marshall, F. E., & Beardmore, A. P. 2015, GRB Coordinates Network, Circular Service, No. 17751, #1 (2015), 17751
- Marshall, F. E., & Krimm, H. A. 2010, GRB Coordinates Network, Circular Service, No. 10394, #1 (2010), 10394
- McLeod, B., & Williams, G. 2009, GRB Coordinates Network, 9370
- Melandri, A., Carter, D., Mundell, C., et al. 2006, GRB Coordinates Network, 5920
- Mészáros, P., & Rees, M. J. 1993, *ApJ*, 405, 278
- Metzger, B. D. 2017, *Living Reviews in Relativity*, 20, 3
- Metzger, B. D., & Berger, E. 2012, *ApJ*, 746, 48
- Metzger, B. D., Martínez-Pinedo, G., Darbha, S., et al. 2010, *MNRAS*, 406, 2650
- Mirabal, N., & Halpern, J. P. 2006, GRB Coordinates Network, 5906
- Morgan, A. N., Cobb, B. E., Klein, C., & Bloom, J. S. 2009, GRB Coordinates Network, 9359
- Naito, H., Sako, T., Suzuki, D., et al. 2010, GRB Coordinates Network, Circular Service, No. 10889, #1 (2010), 10889
- Nakar, E. 2007, *PhR*, 442, 166
- Nicuesa Guelbenzu, A., Klose, S., Greiner, J., et al. 2012, *A&A*, 548, A101
- Nysewander, M., Fruchter, A. S., & Pe’er, A. 2009, *ApJ*, 701, 824
- Perley, D. A., Kislak, M., & Ganeshalingam, M. 2009, GRB Coordinates Network, 9372
- Pian, E., D’Avanzo, P., Benetti, S., et al. 2017, *Nature*, doi:10.1038/nature24298
- Planck Collaboration, Ade, P. A. R., Aghanim, N., et al. 2016, *A&A*, 594, A13
- Poole, T. S., & Troja, E. 2006, GRB Coordinates Network, 5069
- Price, P. A., Berger, E., Fox, D. B., Cenko, S. B., & Rau, A. 2006, GRB Coordinates Network, 5077
- Rosswog, S. 2005, *ApJ*, 634, 1202
- Rosswog, S., Ramirez-Ruiz, E., & Davies, M. B. 2003, *MNRAS*, 345, 1077
- Rosswog, S., Thielemann, F. K., Davies, M. B., Benz, W., & Piran, T. 1998, in *Nuclear Astrophysics*, ed. W. Hillebrandt & E. Muller, 103
- Rowlinson, A., Wiersema, K., Levan, A. J., et al. 2010, *MNRAS*, 408, 383
- Rumyantsev, V., Karimov, R., Salyamov, R., et al. 2006, GRB Coordinates Network, 5184
- Rumyantsev, V., Shakhovkoy, D., & Pozanenko, A. 2010, GRB Coordinates Network, Circular Service, No. 10456, #1 (2010), 10456
- Ryan, G., van Eerten, H., MacFadyen, A., & Zhang, B.-B. 2015, *ApJ*, 799, 3
- Sari, R., Piran, T., & Narayan, R. 1998, *ApJL*, 497, L17
- Savchenko, V., Ferrigno, C., Kuulkers, E., Author, A. N., & Author, A. N. 2017, *ApJ*
- Schlaflly, E. F., & Finkbeiner, D. P. 2011, *ApJ*, 737, 103
- Siegel, M. H., & Beardmore, A. P. 2009, GRB Coordinates Network, 9369
- Smartt et al. 2017, *Nature*, in press
- Stratta, G., D’Avanzo, P., Piranomonte, S., et al. 2007, *A&A*, 474, 827
- Tanvir, N. R., Levan, A. J., Fruchter, A. S., et al. 2013, *Nature*, 500, 547
- Tanvir, N. R., Levan, A. J., González-Fernández, C., et al. 2017, doi:10.3847/20418213/aa90b6

- Tauris, T. M., Kramer, M., Freire, P. C. C., et al. 2017, *ApJ*, 846, 170
- Troja, E., Sakamoto, T., Cenko, S. B., et al. 2016, *ApJ*, 827, 102
- Troja, E., Butler, N., Watson, A. M., et al. 2017, GRB Coordinates Network, Circular Service, No. 21051, #1 (2017), 21051
- Tunnicliffe, R. L., Levan, A. J., Tanvir, N. R., et al. 2014, *MNRAS*, 437, 1495
- Utdike, A. C., Bryngelson, G., & Milne, P. A. 2009, GRB Coordinates Network, 9361
- von Kienlin, A., Meegan, C., Goldstein, A., et al. 2017, GRB Coordinates Network, 21520
- Yang, B., Jin, Z.-P., Li, X., et al. 2015, *Nature Communications*, 6, 7323